Astron. Astrophys. 316, 435–440 (1996)

ASTRONOMY
AND
ASTROPHYSICS

Generation of plasma turbulence and radio emission at the front of interplanetary MHD shocks

V.G. Ledenev

Institute of Solar-Terrestrial Physics, P.O. Box 4026, 664033, Irkutsk, Russia

Received 18 August 1995 / Accepted 24 February 1996

Abstract. Based on spectral observations of turbulence and radio emission in the interplanetary medium from the Ulysses spacecraft, we describe processes responsible for the formation of energetic particle fluxes, the generation of Langmuir and ion acoustic turbulence, and the radio emission at the front of a quasi-perpendicular MHD shock wave. It is shown that an important role in the production of energetic particle fluxes and the generation of emission is played by a collisionless density jump in the shock structure that corresponds to a nonlinear ion acoustic wave.

Key words: MHD – shock waves – Sun: radio radiation – solar wind – interplanetary medium

1. Introduction

A significant fraction of shocks that propagate in the solar wind, are quasi-perpendicular shock waves, i.e., those which propagate at angles to the magnetic field greater than 45–50°. The structure of such shocks was studied in considerable detail by Sagdeev (1964) and Karpman (1963). Subsequent studies of reasonably strong shocks showed that one of the main structural elements is a nonlinear ion acoustic shock which features a density jump without a temperature jump on a scale of ~ 10 Debye radii. In the following such shocks will be referred to as ion acoustic shocks. The existence of such shocks, both as single entities and as structural elements of more complicated (supercritical) shocks, was confirmed theoretically and experimentally in papers by Alikhanov et al. (1971), Eselevich et al. (1971), and Ledenev (1990). The presence of a sharp density jump at the shock front substantially modifies the formation process of energetic particle fluxes and, hence, the generation of plasma turbulence and radio emission. As shown by Alikhanov et al. (1971), a region of intense ion acoustic turbulence can be produced behind the ion acoustic jump. This is indeed confirmed by spacecraft observations (Lengyel-Frey et al. 1992; Burton et al. 1992). These same observations indicate that the region of ion acoustic turbulence occupies an unexpectedly large volume. If it is assumed that the principal ion acoustic damping mechanism is Landau damping by the electrons, then the region of turbulence should have a scale of $\sim 10^2$ wavelengths (Kaplan & Tsytovich 1972). With a characteristic wavelength of ~ 10 Debye radii, a solar wind density of $\sim 1\,\mathrm{cm}^{-3}$ and a temperature of $\sim 10^5$ K, the size of the turbulent region is $\sim 10^6$ cm. If the shock velocity $U_{sh} \sim 10^8\,\mathrm{cm\,s}^{-1}$, then the spacecraft would be within the turbulent region for $\sim 10^{-2}$ s. Actually, however, the duration of the intense ion acoustic turbulence behind the shock front is about an hour (Lengyel-Frey et al. 1992). This means that the turbulence is sustained by some instability.

The generation of plasma turbulence and emission in interplanetary shocks was considered in many papers (see, for example, Ledenev 1977; Krasnoselskikh et al. 1985; Galeev et al. 1988). These publications, however, neglected the possible formation of ion acoustic density jumps at such shock fronts. The objective of this paper is to describe the generation of plasma turbulence and radio emission at the front of an MHD shock wave in the solar wind. Allowance is made for the formation of a density jump corresponding to an ion acoustic shock.

2. The structure of MHD shocks in the solar wind

Let us consider the particular events observed by the Ulysses spacecraft on April 7 and May 27, 1991. On those days the spacecraft observed shocks associated with different types of plasma turbulence and radio emission (Lengyel-Frey et al. 1992; Hoang et al. 1992). The MHD parameters of the two shocks were similar: the magnetic Mach numbers were 3.6 and 2.9, the angles between normal to the front and the magnetic field direction were 80 – 90° and 65–70°, and the density jumps were 2.6 and 2.3, respectively.

Shock wave structure is dependent on the relationship between electroconductivity, heat conduction and viscosity (Kennel 1988; Liberman & Velikovich 1986). The typical scales in the solar wind are determined by the magnetic Reynolds number (the scale of electro-conductivity) $R_m = c^2/4\pi\sigma|U_{sh}| \sim 10^{-2}$ cm, and the scale of heat conduction $R_v = K/c_v\rho_1|U_{sh}| \sim 10^{14}$ cm, where c is the speed of light, σ is the electroconductivity, K is the thermal conductivity, c_v is the specific

heat, and ρ_1 is the unperturbed density of the medium. Viscosity in the solar wind has the same typical scale as the heat conduction.

The small scale of electro-conductivity ($R_v \gg R_m$) signifies an almost totally frozen-in condition of the magnetic field to the plasma. With such high electro-conductivity and heat conductivity, the structure of the shock front must be determined either by dispersion and nonlinearity effects (a laminar collisionless shock) or by collective effects (a turbulent shock) (Sagdeev 1964). When small-scale turbulence develops within the shock front, the scale of electro-conductivity is substantially larger, while the scales of heat conduction and viscosity are significantly smaller than the above estimates. Nevertheless, even for this case, it follows from the above estimates that the largest scale determining the shock structure will be the scale of thermal conductivity. In a quasiperpendicular shock wave this scale is limited by the magnetic field and is roughly given by $R_v \sim U_{sh}/\omega_{hi}$ (Galeev et al. 1988), where ω_{hi} is the ion cyclotron frequency. For a magnetic field $B \sim 10^{-5}$ G and a density $n \sim 1$ cm^{-3} we have $R_v \sim 10^8$ cm. It is assumed that the heating must be ensured by some small-scale instability such as the excitation of ion sound.

Next in the hierarchy of scales in the solar wind is the characteristic dispersion length. For the fast MHD wave considered here, this length is determined by those values of frequency ω and wave number k, for which the dispersion law, i.e. the relationship $\omega = \omega(k)$, departs appreciably from linearity. This is $R_d \sim c\cos(\Theta_1)/\omega_{pi}$ for a quasi-perpendicular shock (Sagdeev 1964), where Θ_1 is the angle between the normal to the front and the magnetic field, and ω_{pi} is the ion plasma frequency. For $n \sim 1$ cm^{-3} we have $R_d \leq 10^7$ cm. If the shock is so strong that heat conduction and viscosity cannot ensure the formation of a shock discontinuity, then a dispersion-induced density and magnetic field jump must form in the front's structure. Since $R_d \ll R_v$, this jump must occur at a constant value of temperature. If this jump also fails to ensure fulfilment of the general relationships for a shock, then the next scale in the structural hierarchy is the Debye radius $r_d \ll R_d$ (for $T \sim 10^5$ K and $n \sim 1\,\mathrm{cm}^{-3}$ we have $r_d \sim 10^3$ cm). A density jump corresponding to an ion acoustic shock can occur on a typical scale of only a few Debye radii (Alikhanov et al. 1971). In this case the magnetic field is unchanged. This is the so-called isomagnetic jump that was investigated experimentally by Eselevich et al. (1971).

We now consider a plausible shock structure in the solar wind. Let the shock propagate along the x-axis. The coordinate system is chosen such that $v_z = B_z = 0$, i.e., the transverse velocity and magnetic field components are directed along the y-axis. The Rankine-Hugoniot relations for a shock in this case may be written as (Landau & Lifshitz 1982)

$$
\begin{aligned}
&[\rho v_x] = 0,\\
&[\rho v_x^2 + P + B_y^2/8\pi] = 0,\\
&[\rho v_x v_y - B_x B_y/4\pi] = 0,\\
&[\rho v_x(v_x^2/2 + v_y^2/2) + \gamma v_x P/(\gamma-1)\\
&\quad + B_y(v_{x1}B_{y1}/4\pi - B_x v_{y1}/4\pi)] = 0,\\
&[v_x B_y - v_y B_x] = 0,
\end{aligned}
\tag{1}
$$

where ρ is the density, P is pressure, and γ is the polytropic index. Square brackets indicate the difference of parameters at an arbitrary point in the front and in the undisturbed region ahead of the shock front designated by the index 1, i.e., $g(x) - g_1$, where $g(x)$ is an arbitrary function. The shock structure can be investigated graphically by plotting curves on the phase plane $r = v_x/v_{x1}$, $b = B_y/B_{y1}$ (Kennel 1988), where v_{x1} is the plasma velocity ahead of the shock front in the shock frame of reference, v_x is the velocity at an arbitrary point in the shock front, B_{y1} is the magnetic field ahead of the shock front, and B_y is the magnetic field at an arbitrary point in the front. The curve defining the locus of points in the plane (r, b) conserves the mass, momentum and energy fluxes from their respective values ahead of the shock front. This curve is obtained from the first four equations of the system (1) and is defined by a quadratic equation for r (Kennel 1988)

$$F(r,b) = Ar^2 + Br + C = 0, \tag{2}$$

where $A = -(\gamma+1)/2(\gamma-1)$, $B = 1/(\gamma-1)M_{s1}^2 + \gamma[1 - (b^2 - \sin^2(\Theta_1))/2M^2]/(\gamma-1)$, $C = -1/(\gamma-1)M_{s1}^2 - 1/2 + [b^2 - \sin^2(\Theta_1) - Y(b - \sin(\Theta_1))^2]/2M^2$, $M_{s1}^2 = \rho_1 v_{x1}^2/\gamma P_1 = v_{x1}^2/C_{s1}^2$, C_{s1} being the sound velocity ahead of the shock front, $M^2 = 4\pi\rho_1 v_{x1}^2/B_1^2 = v_{x1}^2/C_{a1}^2$, C_{a1} being the Alfven velocity ahead of the shock front, and $Y = 1 - 1/M_{I1}^2$, $M_{I1}^2 = 4\pi\rho_1 v_{x1}^2/B_x^2$. It is implied here that the component B_x is conserved at the shock front. The points (r_1, b_1) and (r_2, b_2), corresponding to the unperturbed state ahead of the shock front and the steady-state behind the front, must lie on the curve $F(r,b)$.

Another curve may be obtained from the fifth equation of the system (1)

$$Z(r,b) = bX - Y\sin(\Theta_1) = 0, \tag{3}$$

where $X = r - 1/M_{I1}^2$. The Eq. (3) defines the points at which Ohm's law of ideal magnetohydrodynamics is satisfied, i.e., $\boldsymbol{E} + [\boldsymbol{vH}]/c = 0$. The steady-state parameters r_2 and b_2 behind the shock front must lie on the intersection of these curves (Kennel 1988), because magnetic field diffusion effects (i.e., finite conductivity effects) as well as effects of other dissipation mechanisms are unimportant behind the shock front. The transition from the state (r_1, b_1) to the state (r_2, b_2), however, can proceed in different ways depending on the relationship of typical scales of different dissipation mechanisms.

As pointed out above, density and magnetic field jumps caused by the dispersion can occur in the shock structure at a constant temperature. In this case, neglecting viscosity, the points that determine the parameters r and b across such a jump must lie on a curve describing an isothermal variation of the parameters:

$$
\begin{aligned}
I_2(r,b) = {} & r^2 - (r_2 + r_2/M_{s2}^2\\
& + (b_2^2 - b^2)/2M^2)r + r_2^2/M_{s2}^2 = 0,
\end{aligned}
\tag{4}
$$

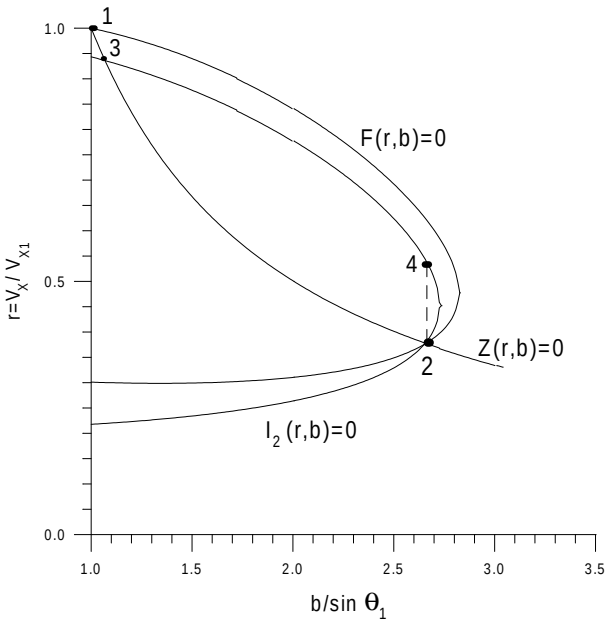

Fig. 1. Graphical solution of the Rankine-Hugoniot relationship for a shock with M = 3.5, Θ_1 = 80°, and β = 1. $F(r, b)$ = 0 is the locus of points where mass, momentum and energy flows are conserved. $Z(r, b)$ = 0 is the curve for a constant electric field, and $I_2(r, b)$ = 0 is the isotherm along which $T = T_2$. The transition from the initial state (point 1) to the final state (point 2) proceeds through points 3 and 4, i.e., through isothermal and isomagnetic jumps

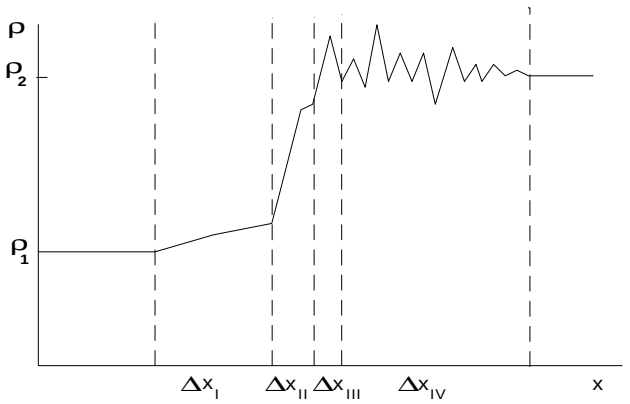

Fig. 2. Qualitative picture of the shock structure. Region I is the footpoint where the main rise in temperature occurs with a minor increase in density and magnetic field ($\Delta x_I \sim U_{sh}/\omega_{hi}$); region II is the isothermal density and magnetic field jump ($\Delta x_{II} \sim c \cdot \cos(\Theta_1)/\omega_{pi}$); region III is the isomagnetic density jump ($\Delta x_{III} \sim 10 r_d$), and region IV is characterized by developed ion acoustic turbulence ($\Delta x_{IV} \sim U_{sh}/\nu$), $\rho_2/\rho_1 \approx 2.6$

where $M_{s2}^2 = \rho_2 v_{x2}^2/P_2$ is the Mach number determined from the isothermal sound velocity and the stream velocity behind the shock front. This equation is obtained from the first two equations of the system (1), assuming that the temperature is constant and is equal to the temperature behind the shock front T_2.

Figure 1 shows a graphical solution of the system of Eqs. (2), (3), (4) for a shock wave propagating at the angle Θ_1 = 80° for M = 3.5. In this case $C_{s1} = C_{a1}$ (the gas-to-magnetic pressure ratio β = 1) and $\gamma = 5/3$. As shown by Kennel (1988), the transition from the undisturbed state (point 1) to the steady state behind the shock front (point 2) will proceed initially along the curve $Z(r, b)$ = 0 (to point 3). In the case of the high conductivity typical of the solar wind, this means that the electric field within the shock front is virtually zero and heat conduction provides the main dissipation mechanism in the initial part of the front (footpoints). Because heat conduction cannot ensure the transition to the steady state behind the shock front (Galeev et al. 1988; Ledenev 1990), however, allowance should be made for factors that ensure a faster variation of parameters of the medium within the shock front. As mentioned above, next in the hierarchy of scales is the dispersion scale R_d. Both the density and the magnetic field increase on this scale. The variation of the parameters now proceeds along the curve $I_2(r, b)$ = 0 (to point 4), along which the temperature equals the steady-state value behind the shock front.

On the other hand, even the dispersion cannot ensure the transition to the steady state behind the shock front. Moving along the curve $I_2(r, b)$ = 0, a point is reached where the magnetic field drops as one moves deeper into the front. In fast shocks, however, the magnetic field can only increase (Kennel 1988). This requires that the transition to the steady state is realized on an even smaller scale, namely a scale of only a few Debye radii corresponding to an ion acoustic isomagnetic density jump. This jump corresponds to the transition from point 4 to point 2 in Fig. 1 and is of the order of ρ_1 in magnitude.

A qualitative picture of the structure of a supercritical quasi-perpendicular shock in the solar wind is shown in Fig. 2. In this figure region I corresponds to the portion of the curve $Z(r, b)$ = 0 up to the intersection with the curve $I_2(r, b)$ = 0. The main dissipation mechanism here is heat conduction. Region II, caused by dispersion and nonlinearity effects, corresponds to the part of the curve $I_2(r, b)$ = 0 from the intersection with the curve $Z(r, b)$ = 0 to the isomagnetic jump (region III). This, in turn, enables the transition to the steady state behind the shock front through the oscillatory region IV. The isomagnetic jump is accompanied by ion acoustic oscillations of large amplitude and by whistler waves which are generated as a result of the nonlinear evolution of fast MHD waves (Galeev et al. 1988). Here, the dissipation is ensured by ions reflected from electric potential jump, and because of Landau damping of ion acoustic and whistler waves or Coulomb collisions.

The calculations show that the ion acoustic potential jump increases with increasing shock Mach number M and decreases slowly with increasing angle Θ_1 between the wave propagation direction and the magnetic field. For example, the jump disappears for a decrease of the Mach number to $M \approx 2.5$ for $\beta \approx 1$. Increasing the Mach number to $M \approx 4.5$, the potential jump increases to such an extent that most of the incoming ion flow is reflected and the laminar structure of the front decays. These

results agree with those derived experimentally by Eselevich et al. (1971).

3. The generation of plasma turbulence and radio emission within the shock front

It is common for ion acoustic turbulence to be excited by a current instability, i.e., in the presence of relative motion between electrons and ions. Current behind the shock front can be maintained by electrons reflected from the electric potential jump within the shock front associated with a density jump. The point here is that electrons moving with a velocity higher than the shock front's velocity will be reflected into the region behind the shock front. In a strong shock, where the stream velocity behind the front is 3/4 of the front's velocity, most electrons will be reflected, the velocity of which exceeds that of directed mass motion behind the front by more than 1/4. The velocity of electrons relative to the ions U_c is defined as the first moment of the distribution function. Using a coordinate system moving with the ions behind the shock front and for $v_{te} \gg U_{sh}$ we obtain

$$U_c = \int v[f_0(v) + f_b(v)]dv = \quad (5)$$
$$1/(\sqrt{\pi}v_{te}) \int_{U_{sh}/4}^{v_{te}} v \exp(-v^2/v_{te}^2)dv,$$

where $f_0(v)$ is the distribution function of ions traveling in the same direction as the shock wave and $f_b(v)$ is the distribution function of reflected electrons. It is assumed here that $\int_{-\infty}^{\infty} v f_0(v)dv = 0$.

We obtain from Eq. (5) $U_c \approx 0.2v_{te}$. This velocity is substantially larger than the threshold velocity for a current instability $v_{cr} \sim v_{ti}$, where v_{ti} is the thermal velocity of the ions (Mikhailovsky 1975). Even allowing for the fact that the velocity component of reflected electrons from a quasi-perpendicular shock directed along magnetic field lines in a quasi-perpendicular shock is substantially smaller than this value, the condition for onset of the instability will be satisfied. The electron distribution function will relax under the action of excited ion acoustic waves to a quasi-stationary state only when the growth rate of oscillations goes to zero. Consequently, ion acoustic turbulence will be sustained not only within the shock front (near the density jump) but also at large distances from it. The damping rate of the current instability is determined by the Coulomb collision frequency ν. For solar wind conditions $\nu \sim 10^{-4}$ s (the damping time is about an hour), which agrees with the observations reported by Lengyel-Frey et al. (1992).

In addition to being reflected into the region behind the shock front, some of the highest-energy electrons will overcome the electric potential jump at the shock front, thus forming a beam. This beam is produced by electrons with an energy large enough for their velocity (after overcoming the potential barrier) to exceed the shock velocity. Since shocks move with velocities less than the thermal electron velocity, such beams do not excite plasma waves when the shock travels along the field. If the shock moves at a reasonably large angle to the magnetic field, however, then the electrons that escape the shock must have a velocity along the field $U \sim U_{sh}/\cos(\Theta_1)$.

Typical shock velocities in the solar wind are 10^7–10^8 cm s^{-1} (Hundhausen 1972). The thermal velocity of electrons $v_{te} \sim 10^8$ cm s^{-1} for $T \sim 10^5$ K. The velocity of electron beams that drive plasma waves must thus be larger than $3v_{te}$ ($3 \cdot 10^8$ cm s^{-1}). Accordingly, the angle Θ_1 for shocks that generate the emission, must be in the range $70° < \Theta_1 < 88°$.

A similar approach to studying the excitation process of Langmuir turbulence at the shock front was developed by Smith (1971). He considered virtually perpendicular shocks (propagation at angles to the magnetic field larger than 86°), however, which have a different laminar structure. Accordingly his results require that electrons escaping from the shock front must have substatially larger velocities and a significantly smaller densities.

Let us now consider the processes within the shock front in greater detail. At this point it is important to note that under solar wind conditions both the ion and electron cyclotron radii are much larger than the Debye radius, namely $r_i \sim 10^7$ cm, $r_e \sim 10^5$ cm, and $r_d \sim 10^3$ cm. Therefore the particles near the ion acoustic jump may be thought of as following rectilinear paths.

As is known (Alikhanov et al. 1971; Eselevich et al. 1971; Ledenev 1990), ahead of the ion acoustic shock front there exists an ion flow reflected from the electric potential jump within this shock front. This ion flow will excite ion acoustic turbulence with a growth rate $\gamma \sim (n_{bi}/n)\omega_{pi}$ (Ivanov 1977), where n_{bi} is the density of the reflected ion flow, and ω_{pi} is the ion plasma frequency. Because the shock velocity (and hence the velocity of the reflected ion flow) is substantially higher than the velocity of sound, ion-sound waves are excited in a direction close to the plane of the shock front. At the same time, as pointed out previously, the escaping electron flow at large angles between the direction of motion of the shock and the magetic field direction also moves nearly parallel to the front's plane and excites Langmuir turbulence predominantly in this direction. This is the most favourable situation for transforming Langmuir waves due to ion acoustic wave excitation into electromagnetic radiation.

It should be noted that, since the group velocity of Langmuir waves is always smaller than the phase velocity, these waves will lag behind the electrons that excite them. A significant fraction of the waves will be overtaken by the shock and reflected from its density jump. This can result in an accumulation of Langmuir turbulence ahead of the shock front and, consequently, a more effective transformation into electromagnetic radiation (Ledenev 1977).

Figure 3 presents a qualitative picture of the electric potential, reflected and escaping particle fluxes and plasma turbulence at the shock front. Note that the potential distribution has essentially the same form as the density profile (Fig. 2).

The reflected ion flow density can be estimated in the following way. General relationships for the quasi-perpendicular ion acoustic jump, with allowance made for the fact that the magnetic field is unchanged, may be written as (Bardakov et al. 1975; Ledenev 1990)

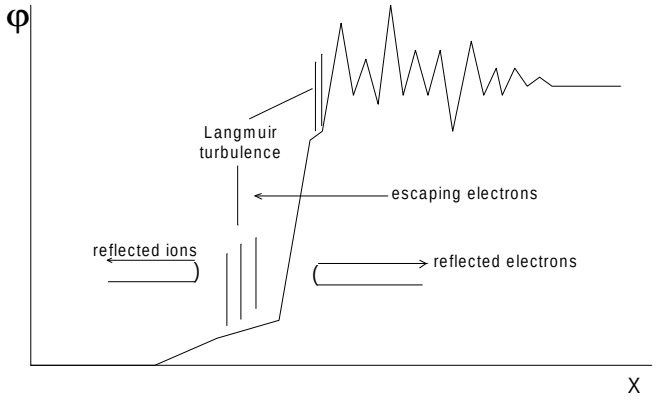

Fig. 3. Qualitative profile of electric potential, showing particle fluxes and plasma turbulence at the shock front

$$
\begin{aligned}
&(n_f - n_r)u_{10} = n_2 u_2,\\
&n_{10}u_s^2\exp(\Psi_1) + (n_f + n_r)u_{10}^2 = n_2 u_2^2 + n_{10}u_s^2\exp(\Psi),\\
&(1/2)u_{10}^2 + \Psi_1 u_s^2 + B_2^2/4\pi(n_f + n_r)m_i =\\
&\qquad (1/2)u_2^2 + \Psi u_s^2 + B_2^2/4\pi n_2 m_i,\\
&n_f + n_r = n_{10}\exp(\Psi_1),\\
&n_2 = n_{10}\exp(\Psi),
\end{aligned}
\tag{6}
$$

where n_{10} is the density ahead of the ion acoustic jump, u_{10} is the stream velocity (in the shock system) immediately ahead of the ion acoustic jump, n_2 and u_2 are the plasma density and velocity behind the shock front, respectively, n_r is the density of reflected ions, n_f is the density of incoming ions at the ion acoustic jump, $\Psi_1 = e\phi_1/T_2$ is the potential produced by reflected ions, $\Psi = e\phi/T_2$ is a total potential drop across the ion acoustic jump, T_2 is the temperature of electrons behind the shock front, $u_s = (T_2/m_i)^{1/2}$, m_i is the mass of an ion, and B_2 is the magnetic field behind the shock front.

The temperature behind the shock front can be determined from the relationship relating the parameters r and b, which, in turn, was obtained from laws of conservation across a shock discontinuity (Kennel 1988)

$$r(1 + 1/M_s^2) = 1 + 1/\tilde{M}_{s1}^2 - (b^2 - sin^2(\Theta_1))/2M^2, \tag{7}$$

where $M_s^2 = v_x^2\rho/P$, $\tilde{M}_{s1}^2 = v_{x1}\rho_1/P_1$. For the calculations performed above (see Fig. 1), we have $r_2 = 0.38$ and $b_2 = 2.62$. A corresponding value of the isothermal Mach number is

$$M_{s2} = [(1/r_2)(1+1/\tilde{M}_{s1}^2 - (b_2^2 - \sin^2(\Theta_1))/2M^2) - 1]^{-1/2}. \tag{8}$$

We obtain from (8) $M_{s2} = 0.84$. The corresponding density jump, as is apparent from Fig. 1 (transition from point 4 to point 2), is $n_2/n_{10} \approx 1.42$. This corresponds to an electron temperature behind the front $T_2 \approx 5T_1$.

From the system of Eqs. (6), in view of the condition of conservation of mass flow $\rho_1 v_{x1} = \rho v_x$, we obtain an estimate of the reflected-ion flow density $n_r/n_{10} \approx 0.3$. The corresponding growth rate of ion acoustic waves is $\gamma_i \sim n_r\omega_{pi}/n$. For $n \sim 1\,\mathrm{cm}^{-3}$ we have $\gamma_i \sim 10^2\ \mathrm{s}^{-1}$. Under solar wind conditions $B \sim 10^{-5}$ G, and the ion cyclotron frequency $\omega_{hi} \sim 10^{-1}$ s $\ll \gamma_i$, i.e., the reflected ions that excite ion sound must follow rectilinear paths. The reflected ions become isotropic in a time $t \sim [\omega_{pi}(n_r/n)(u_s/u_r)^2]^{-1}$, where u_r is the velocity of the reflected ion flow (Ivanov 1977). In our case $\omega_{pi} \sim 10^3\ \mathrm{s}^{-1}$ and a typical value of $u_s/u_r \sim 10^{-1}$. When $n_r/n \sim 10^{-1}$ we obtain $t \sim 1$ s, i.e., the reflected ions become isotropic in a time shorter than the cyclotron period. The corresponding energy density of the ion acoustic waves (Ivanov 1977) is $W^s \sim n_r m_i u_r^2(u_s/u_r) \sim 10^{-11}\,\mathrm{erg\,cm}^{-3}$.

Langmuir waves, as pointed out above, are excited by an electron beam with sufficient energy to overcome the electric potential jump and then outrun the shock, even while moving along magnetic field lines. With a sufficiently large angle between the direction of motion of the shock and the magnetic field, the velocity of the electron beam will be substantially larger than the thermal velocity, and a beam instability will develop. In this case, escaping electron beams can form at both the dispersion-induced jump and the ion acoustic jump. In the former case the beam forms and excites an instability largely ahead of the shock front, and corresponding emission will be observed near the plasma frequency determined by the density ahead of the front (Lengyel-Frey et al. 1992; Hoang et al. 1992). In the latter case, as a consequence of the small thickness of the ion acoustic jump compared with the electron cyclotron radius, the beam is produced within the front near its rear boundary, and the corresponding emission will be observed near the plasma frequency determined by the density behind the shock front (Lengyel-Frey et al. 1992; Hoang et al. 1992).

The energy density of the plasma waves excited by an electron beam can be estimated by considering the boundary-value problem of stationary injection of the beam into a half-space filled with a plasma (Vedenov & Ryutov 1972). In this case the energy density of Langmuir waves is $W^l \approx mn_b v_b^4/15v_{te}^2 \sim n_b m v_b^2$.

The electron density in the beam n_b can be estimated by assuming the electron distribution function to be Maxwellian and the value of the density jump corresponding to an ion-acoustic shock to be $\sim n_1$. The Landau damping of plasma waves is unimportant for electrons with velocities larger than $3v_{te}$ ($v_b > 3 \cdot 10^8\,\mathrm{cm\,s}^{-1}$), i.e., when the beam is produced from electrons with energies an order of magnitude higher than the thermal energy within the shock front. With a Maxwellian distribution, the electron beam density will be $n_b \sim 10^{-2}n_1$. Allowing for the fact that these electrons travel largely along the field, they must be $n_b \sim 10^{-3}n_1$. This represents a lower bound because the real distribution function in a shock differs from a Maxwellian primarily by the presence of high-energy electron tails. Hence $W^l \sim 10^{-13}\,\mathrm{erg\,cm}^{-3}$.

It may be suggested that plasma wave energy densities of the same order of magnitude are also achieved at a dispersion jump, despite the fact that the potential jump and the corresponding density jump are larger. This is attributed to the significantly larger thickness of the dispersion jump (typically of the order of the electron cyclotron radius) and to a significant 'isotropiza-

tion' of the electrons during the interaction with ion acoustic turbulence.

Radio emission is generated when Langmuir and ion acoustic waves merge together. This process is governed by the equation (Tsytovich 1967)

$$dW_k^t/dt = \gamma_t W_k^l, \tag{9}$$

where $\gamma_t \approx (\omega_{pe}^3/nmv_{te}c^3)W_k^s/k$, and W_k^l and W_k^s are the spectral energy densities of Langmuir and ion-sound waves, respectively. Using the above energy density estimates for Langmuir and ion acoustic waves, and assuming wave numbers for Langmuir waves $k \sim \omega_{pe}/v_b \sim 10^{-3}\,\mathrm{cm}^{-1}$, and ion acoustic waves $k_s \sim r_D \sim 10^{-3}\,\mathrm{cm}^{-1}$ and electromagnetic waves $k_t \sim 10^{-5}\,\mathrm{cm}^{-1}$, we obtain an energy density of electromagnetic waves $W^t \sim W_k^l \cdot k_t \cdot t_{rel}^{-1} \cdot \Delta t \sim 10^{-17}\,\mathrm{erg\,cm}^{-3}$, where Δt is the enhancement time of electromagnetic waves ($\Delta t \sim R_d/c \sim 10^{-3}$ s), and t_{rel} is the time of quasi-linear relaxation ($t_{rel} \sim 10\gamma_t^{-1} \sim 10^{-1}$ s). Here, it is assumed that the growth rate γ_t is determined by the largest build-up time of all wave modes, namely by the enhancement time of Langmuir waves or by a quasi-linear relaxation of the electron beam. This estimate for the energy density of the electromagnetic waves is in good agreement with observations (Hoang et al. 1992).

4. Conclusion

Investigating the shock conservation relations at an MHD discontinuity, it is shown that the transition to a steady-state behind the front of a quasi-perpendicular shock wave in the range of magnetic Mach numbers $2.5 < M < 4.5$ can be achieved only with a density jump corresponding to an ion acoustic shock. Ions reflected from this jump in the direction of motion of the shock and electrons reflected in a backward direction excite intense ion acoustic turbulence. At the same time, electrons that lead the shock will excite Langmuir turbulence which transforms to electromagnetic radiation by scattering from ion acoustic waves. This model provides a reasonable explanation of the spectrum and intensity of plasma turbulence and the electromagnetic radiation observed in interplanetary space.

Acknowledgements. I am grateful to Mr. V.G. Mikhalkovsky for his assistance in preparing the English version of the manuscript and Drs. V.V.Grechnev and A.S. Leonovich for help in preparing of LaTeX version.

References

Alikhanov S.G., Belan V.G., Kichigin G.N., Chebotayev P.Z., 1971, Zh. Eksp. Teor. Fiz. 60, 982

Bardakov V.M., Morozov A.G., Shukhman I.G., 1975, Fizika Plazmy 1, 955 (in Russian)

Burton M.E., Smith E.J., Goldstein B.E. et al., 1992, J. Geophys. Res. Lett., 19, 1287

Eselevich V.G., Eskov A.G., Kurtmullaev R.Kh., Malyutin A.I., 1971, Zh. Eksp. Teor. Fiz. 60, 2079

Galeev A.A., Krasnoselskikh V.V., Lobzin V.V., 1988, Fizika Plazmy 14, 1192 (in Russian)

Hoang S., Pantellini F., Harvey C.C., et al., 1992, In: Marsch E., Schwenn R. (eds.) Solar Wind Seven, Pergamon Press, Oxford, p. 465

Hundhausen A.J., 1972, Coronal Expansion and Solar Wind, Springer-Verlag, Heidelberg, New York, p. 203

Ivanov A.A., 1977, The Physics of Strongly Nonequilibrium Plasma, Nauka, Moscow, p. 348 (in Russian)

Kaplan S.A., Tsytovich V.N, 1972, Plasma Astrophysics, Nauka, Moscow, p. 440

Karpman V.I., 1963, Zh. Tekh. Fiz. 33, 959

Kennel C.F., 1988, J. Geophys. Res. 93, 8545

Krasnosel'skikh V.V., Kruchina E.N., Thejappa G., Volokitin A.S., 1985, A&A 149, 323

Landau L.D., Lifshitz E.M., 1982, Electrodynamics of Continuous Media, Nauka, Moscow, p. 620

Ledenev V.G., 1977, Sov. Astron. Lett. 3(3), 144

Ledenev V.G., 1990, Zhurnal Prikladnoi Mekhaniki i Tekhnicheskoi Fiziki, No. 2, p. 17

Lengyel-Frey D., MacDowell R.J., Stone R.G., et al., 1992, In: Marsch E., Schwenn R. (eds.) Solar Wind Seven, Pergamon Press, Oxford, p.477

Liberman M.A., Velikovich A.L., 1986, Physics of Shock Waves in Gases and Plasmas, Springer-Verlag, New York

Mikhailovsky A.V., 1975, The Theory of Plasma Instabilities, v.1, Nauka, Moscow, p. 272

Sagdeev R.Z., 1964, In: M.A. Leontovich (ed.) Voprosy teorii plazmy, v.4, Atomizdat, Moscow, p. 20 (in Russian)

Smith D.F., 1971, ApJ 170, 559

Tsytovich V.N., 1967, Nonlinear Effects in Plasma, Nauka, Moscow, p. 288

Vedenev A.A., Ryutov D.D., 1972, In: M.A. Leontovich (ed.) Voprosy teorii plazmy, v.6, Atomizdat, Moscow, p. 3 (in Russian)